optica

Programmable generation of terahertz bursts in chirped-pulse laser amplification

Vinzenz Stummer,[1,†] Tobias Flöry,[1,2,†] Gergő Krizsán,[3,†] Gyula Polónyi,[3,4]
Edgar Kaksis,[1] Audrius Pugžlys,[1,5] János Hebling,[3,4] József András Fülöp,[3,4,6] and
Andrius Baltuška[1,5,*]

[1]Photonics Institute, TU Wien, Gusshausstraße 27-387, A-1040 Vienna, Austria
[2]Institute of Theoretical Chemistry, University of Vienna, Währingerstraße 17, A-1090 Vienna, Austria
[3]Szentágothai Research Centre, University of Pécs, Ifjúság ú. 20, H-7624 Pécs, Hungary
[4]MTA-PTE High-Field Terahertz Research Group, Ifjúság ú. 6, H-7624 Pécs, Hungary
[5]Center for Physical Sciences & Technology, Savanoriu Ave. 231, LT-02300 Vilnius, Lithuania
[6]ELI-ALPS, ELI-HU Nonprofit Ltd., Wolfgang Sandner u. 3, H-6728 Szeged, Hungary
*Corresponding author: andrius.baltuska@tuwien.ac.at

Amplified bursts of laser pulses are sought for various machining, deposition, spectroscopic, and strong-field applications. Standard frequency- and time-domain techniques for pulse division become inadequate when intraburst repetition rates reach the terahertz (THz) range as a consequence of inaccessible spectral resolution, requirement for interferometric stability, and collapse of the chirped-pulse amplification (CPA) concept due to the loss of usable bandwidth needed for safe temporal stretching. Avoiding the burst amplification challenge and resorting to lossy post-division of an isolated laser pulse after CPA leaves the limitations of frequency- and time-domain techniques unsolved. In this Letter, we demonstrate an approach that successfully combines amplitude and phase shaping of THz bursts, formed using the Vernier effect, with active stabilization of spectral modes and efficient energy extraction from a CPA regenerative amplifier. As proof of concept, the amplified bursts of femtosecond near-infrared pulses are down-converted into tunable THz-frequency pulses via optical rectification.

1. INTRODUCTION

Laser pulse bursts with high energies up to multi-millijoules (mJ) at various intraburst repetition rates have already found their way into a number of applications, such as materials processing [1], pulsed laser deposition [2], laser induced breakdown spectroscopy (LIBS) [3], and seeding of free electron lasers [4]. However, for high intraburst repetition rates, there exists a fundamental limitation of the achievable burst energy in conventional chirped-pulse amplification (CPA) systems, which prevents access to the multi-mJ regime. This limitation originates from the buildup of spectral modes resulting from interpulse spectral interference, which are mapped into the time domain as strong spikes on the temporal intensity profile of the stretched overlapping pulses circulating in the laser amplifier. The motivation of this work is to propose and demonstrate an approach that allows suppression of spectral mode formation by programming phases of individual pulses at terahertz (THz) intraburst repetition rates directly in the time domain.

Time-domain methods relying on electro-optic or acousto-optic modulators (AOMs) [5–7] are by far too slow to reach the THz regime. By using Fourier-synthesis methods or direct space-to-time conversion [8], a pulse can be shaped with masks, programmable spatial light modulators [9], or arrayed-waveguide gratings [10–13]. However, this approach is inadequate for versatile burst formation by broadband pulse shaping at THz modulation frequencies due to an impossibly high number of spectral channels needed to satisfy both the spectral bandwidth and resolution criteria. Consequently, the programmable time spacing for femtosecond pulses is restricted to several picoseconds, making entire classes of experiments, such as studies of a rotational molecular response, inaccessible to existing spatial light modulators. Interferometric pulse division and re-stacking methods can provide THz modulation frequencies, but their flexibility and programmability is strongly restricted [14].

In this work, the Vernier effect [15] is utilized in a burst generation method, which is capable of providing arbitrarily short temporal separations Δt of pulses as determined by the difference of the roundtrip time t_{MO} of a master oscillator (MO) and the roundtrip time t_{RA} of a regenerative amplifier (RA). The enormous potential of the Vernier effect is explained by the following advantages: 1. By adjusting the difference in cavity length, the pulse

separation can be tuned continuously down to within the duration of a single compressed pulse. 2. The number of pulses per burst can be chosen arbitrarily, as the upper limit on the burst duration is only limited by the time of the cavity roundtrip and Pockels cell (PC) switching. 3. Intraburst pulse shaping can be decoupled from the burst formation process by shaping pulses before injection into the RA. This enables direct time-domain amplitude and phase control at the THz intraburst repetition rate using slow modulators operating at the MO repetition rate.

2. SUPPRESSION OF INTERFERENCE EFFECTS

Burst-mode amplification is frequently perceived as more efficient compared to single-pulse amplification, because the energy stored in the laser material is shared among N pulses. Therefore, the effective pulse duration is increased by a factor of N in the amplifier, and the extractable energy scales with the square root of the pulse number $\sqrt{N}$, an advantage which is explored in many variants of divided-pulse amplification. This is comparable to CPA, where the energy extraction scales with the square root of the stretched-pulse duration $\sqrt{\tau}$ [16–19].

However, no such advantage exists for pulse separations that are significantly shorter than the stretched-pulse duration in conventional CPA. On the contrary, as illustrated in Fig. 1, the energy safely extractable from a chirped pulse amplifier rapidly drops as N increases. A burst composed of N spectrally overlapping pulses with constant phase offsets exhibits discrete spectral lines, spaced at the intraburst repetition rate, as an outcome of spectral interference. Therefore, compared to single-pulse operation, the peak spectral intensities inside the amplifier dramatically increase by a factor of N^2 for the same output energy. This N^2 scaling reflects the growth of temporal peak intensities, as a result of frequency-to-time mapping at high chirp rates. To resolve this detrimental consequence of mode formation, we employ a phase-scrambling technique, which inhibits constructive interference by applying programmable phase offsets $\Phi_{\text{offset},n}$ to each individual intraburst pulse. These offsets are combined with a constant pulse-to-pulse

phase slip $\Delta\Phi_{\text{slip}} = k\Delta L = k(L_{\text{MO}} - L_{\text{RA}})$, which follows from the mismatch of the MO-RA cavity roundtrip lengths ΔL, with k being the wavenumber. The phase differences between subsequent intraburst pulses become

$$\Phi_n - \Phi_{n-1} = \Delta\Phi_{\text{slip}} + (\Phi_{\text{offset},n} - \Phi_{\text{offset},n-1})$$

$$(n = 2, 3, \dots, N). \tag{1}$$

By an appropriate choice of the phase offsets, the burst spectrum is shaped to maximally resemble the single-pulse spectrum. At a given spectral peak intensity, the burst-mode extractable energy can be benchmarked against the single-pulse case by considering the spectral area that is covered by the burst. In Fig. 1, which is based on numerical calculations, we show that the energy that can be extracted is much higher when applying the phase-scrambling technique.

We reproduced amplified burst spectra by applying a numerical model, in which we assumed for every intraburst pulse the measured single-pulse spectrum after amplification and the phase offsets as they were programmed to the AOM, and used the pulse-to-pulse phase slip as the only fit parameter. As can be seen in Fig. 2, the numerical calculation is close to our experimental results, with a slight overestimation of the side wings in the phase-scrambled case. At this point, we emphasize the effect of phase modulation or change in pulse number on the seed burst spectrum. Together with the wavelength-selective gain profile of the amplifier, this leads to a variation of output burst energy at a given pump rate.

We explored the potential of our approach by determining the maximum extractable energy achievable by phase-scrambling as a function of the burst pulse number N and calculated this energy relative to the extractable single-pulse energy under the assumption of identical Gaussian spectra for intraburst pulses (Fig. 3). We determined optimized sets of phase offsets in two ways: first, by a numerical optimization algorithm (limited-memory Broyden–Fletcher–Goldfarb–Shanno boundaries, L-BFGS-B) [20] and, second, by calculating the global maximum energy with restricting the phase offset to zero and π (π-mod). Without
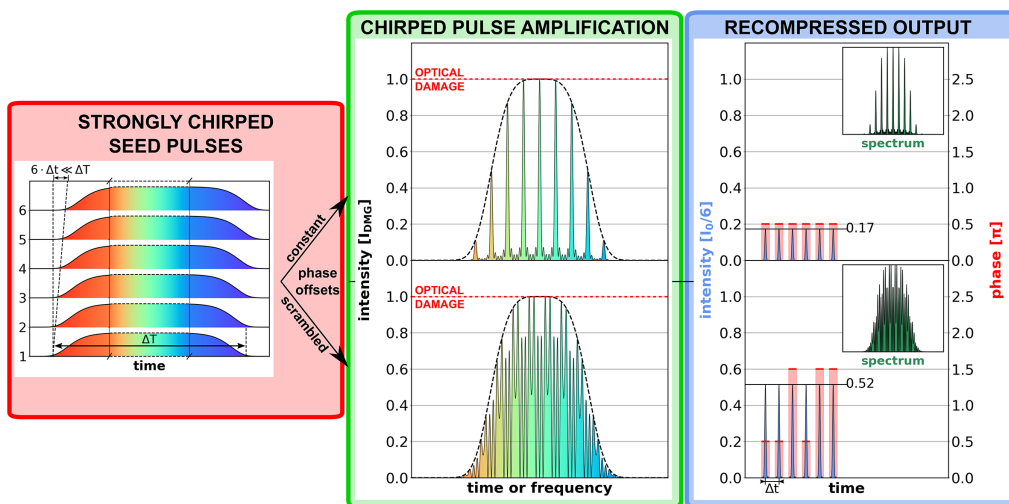
Fig. 1. Safe chirped amplification of a burst utilizing phase-scrambling. Left: composition of the seed burst from strongly chirped overlapping intraburst pulses. Middle: spectral or temporal intensity of the amplified strongly chirped burst, normalized to the optical damage threshold intensity I_{DMG} of the RA, with pronounced spectral modes in the case of constant phase offsets (middle, upper panel). This can be avoided by programmable scrambling of the phase offsets (middle, lower panel). An amplified single chirped pulse is shown for comparison (black dashed line). Right: time-domain representation of intensity (blue) and phase (red) after compression with the intensity normalized to I_0/N, with I_0 being the maximum output peak intensity of a single pulse and N pulse number. The inset shows the spectrum (green).
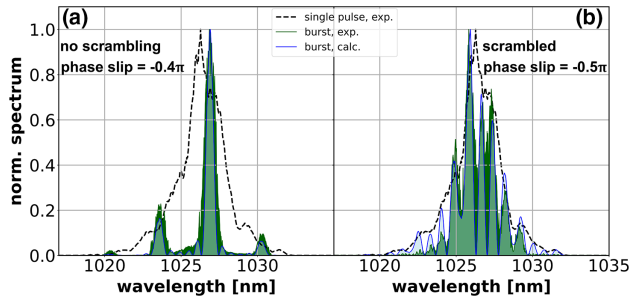
Fig. 2. Comparison of experimentally measured spectra, both non-scrambled and scrambled, with our numerical model. Experimental results showing the single-pulse spectrum (black dashed line) and the burst spectra for $N = 6$ (green) with the programmable phase offset being (a) constant and (b) scrambled with π phase shifts, compared to the numerically calculated spectrum (blue lines).
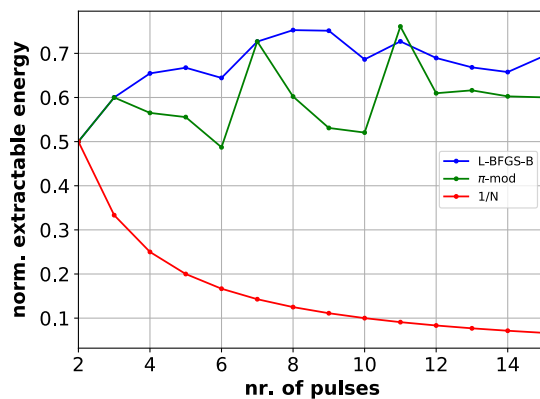
Fig. 3. Maximum extractable energy without exceeding the optical damage threshold in burst mode normalized to the single-pulse case versus pulse number N. Calculation with a programmable phase offset that is constant (red), optimized by a numerical L-BFGS-B algorithm (blue) and the global maximum when allowing only zero or π phase offsets (green).

phase-scrambling, the maximum extractable energy is inversely proportional to the pulse number. In contrast, for both illustrated phase-scrambling cases, the relative extractable energy stays reliably above 50% and approaches approximately 70% of the maximum single-pulse energy for higher pulse numbers.

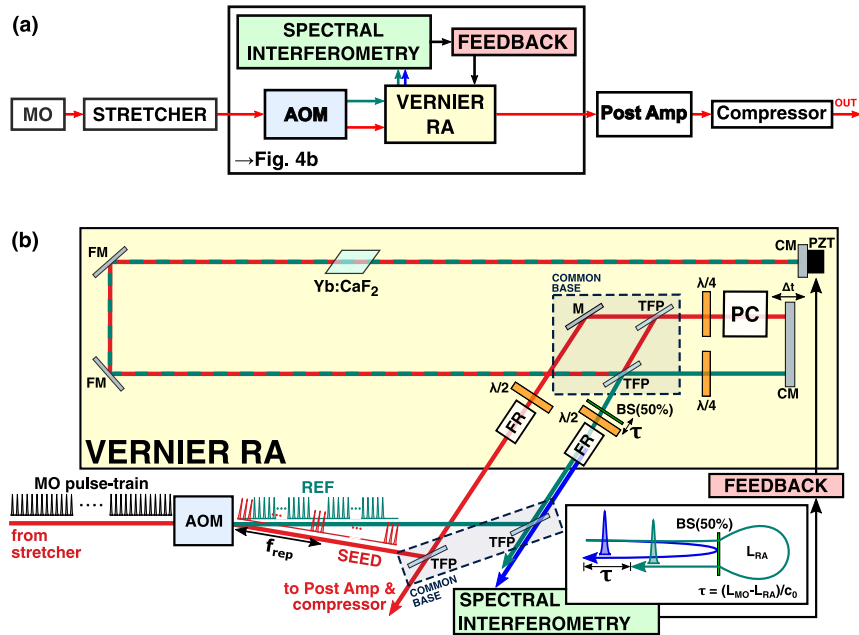## 3. EXPERIMENTAL SETUP & RESULTS

A. Near-infrared Burst Amplification

Our Vernier RA setup with intraburst phase slip stabilization is presented in Fig. 4. A periodic pulse train is generated from a Yb : KGd(WO$_4$)$_2$ (Yb:KGW) MO with $f_{MO} = 76$ MHz repetition rate, and the pulses are stretched to approximately 150 ps. For the control of individual pulse amplitudes and phases, an AOM is used. The RA PC operates synchronously with the AOM to accumulate the AOM-diffracted seed pulses in the RA cavity. The function of the PC is modified compared to conventional on/off operation by allowing it to switch to an intermediate PC voltage level for pulse accumulation in the cavity, enabling subsequent seed pulses to enter the cavity, while only partially coupling out already accumulated pulses. The PC voltage is set such that the induced losses are compensated by the roundtrip gain, resulting in uniform burst formation. After the desired number of burst pulses

is reached, the PC voltage is raised further to lock and amplify the burst in the cavity. In order to reach multi-mJ energies, the burst is amplified further in a cryogenically cooled Yb : CaF$_2$ booster RA before it is recompressed to 250 fs by a grating compressor. Burst energies of up to 4 mJ were achieved for 2, 4, and 6 pulses. With the same system, single 5 mJ pulses were generated under similar pumping conditions. However, we did not amplify up to the optical damage threshold. Due to the already mentioned points regarding the spectral selectivity of the gain profile, extracted energy at a certain pump level in burst mode cannot be directly compared to single-pulse operation.

Thermal drift and mechanical vibrations can lead to variations in the cavity roundtrip times, thus affecting the intraburst phase slip and the burst spectrum. This leads to unstable phase offsets preventing a useful realization of the phase-scrambling technique, which requires a proper choice of programmed intraburst phases. Therefore, an active feedback control of the cavity length difference was implemented to compensate for such influences (Fig. 5), without the need of an external reference cavity. This method can be seen as an intraburst counterpart of widely established carrier envelope phase (CEP) stabilization techniques [21–23] that, to date, have been applied to continuous pulse trains of mode-locked oscillators. The differential cavity length drift is stabilized by monitoring the spectral interference of consecutive pulses in the non-diffracted beam at the MO repetition rate f_{MO} (Fig. 4). One of the interfering reference pulses is reflected off a beamsplitter, and the other one undergoes one complete RA roundtrip. The active feedback control is realized as a software-implemented proportional–integral–derivative (PID) controller with a piezo-electric transducer (PZT) attached to one of the mirrors in the RA cavity and by evaluating the reference interference spectrum.

B. Burst-driven Terahertz Generation

As to demonstrate control over THz intraburst repetition rates, we perform generation of THz pulse bursts by optical rectification in LiNbO$_3$ using tilted-pulse-front pumping (TPFP) [24,25]. With near-infrared (NIR) bursts of 2.5 mJ, we achieved THz burst energies of up to 4 μJ, thus attaining a conversion efficiency of around 0.16% (see Supplement 1 Fig. S16). Second-harmonic generation (SHG) autocorrelations of the NIR burst driver and recorded linear autocorrelations of generated THz transients using a Michelson interferometer together with spectra retrieved by Fourier transformation can be seen in Fig. 6. The measurements were performed for variable pulse spacing with fixed-pulse number [Fig. 6(a), $N = 6$] and for variable pulse number with fixed-pulse spacing [Fig. 6(b), $\Delta t = 3$ ps]. As expected, the continuously tunable intraburst repetition rate is determined by the inverse pulse spacing $1/\Delta t$, translating into the lowest-order THz frequency, whereas the bandwidth Δf of the generated THz peak scales inversely to the product of the pulse number and spacing $1/(N \cdot \Delta t)$, with values $\Delta f_{N=2} = 138$ GHz, $\Delta f_{N=4} = 58$ GHz, and $\Delta f_{N=6} = 50$ GHz. The spectra exhibit a high spectral contrast that progressively improves with N. Higher harmonics of the THz signal are observed as well, in accordance with the Fourier transformation of a windowed-pulse train. The THz pulse source demonstrated here offers a unique combination of versatile pulse shaping capability and scalability to high energies, thereby surpassing many other methods [26,27].

Fig. 4. Vernier setup. (a) Block diagram of the complete experimental setup comprising a MO (Light Conversion Flint), two RAs (one as preamplifier, one as booster amplifier), a stretcher, a compressor, and an AOM for separating seed and reference pulses. The RAs are home-made table-top systems, both with Yb : CaF$_2$ crystals as active elements, where, for the booster amplifier, the crystal was cryo-cooled to approximately 100 K. (b) More detailed scheme of the Vernier RA with burst formation and phase slip stabilization. Pulses with a sufficiently long temporal spacing are diffracted from the MO pulse train (black) with an AOM, which enables individual amplitude and phase modulation. The diffracted pulses (red) are used as the burst seed, and the non-diffracted pulses (turquoise) are used as high-repetition-rate reference for measuring the phase slip drift. The seed pulses are accumulated and amplified in the RA cavity. Inset: concept of the interferometric phase slip drift measurement. The reference pulses are split into two pulses. One (blue) is reflected from a beamsplitter (BS), and another (turquoise) fulfills a roundtrip in the RA cavity. The timing is set such that the transmitted part of a pulse spectrally interferes with the reflection of the next pulse.
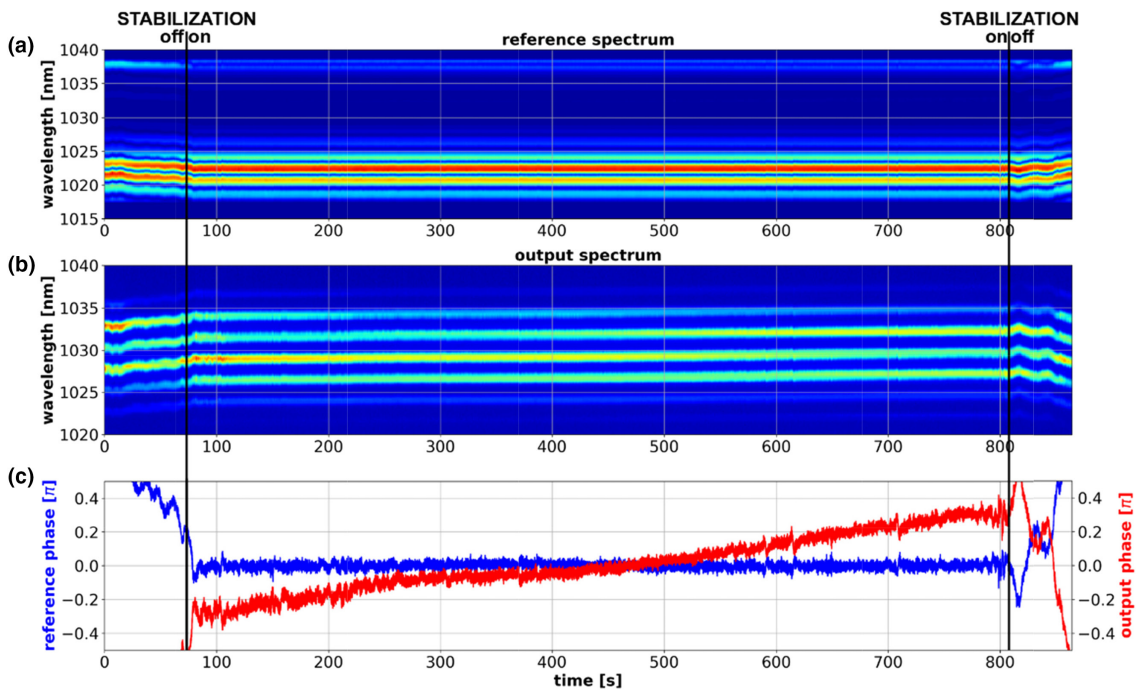
Fig. 5. Intraburst phase slip stabilization results. Spectrum over time of (a) an interferometric reference (in-loop) and (b) the output burst ($N = 4$, $\Delta t = 3$ ps, out-of-loop). (c) Phase of the interferometric reference (blue) and the intraburst phase slip (red) over time. The intraburst phase slip stabilization is realized by controlling the cavity length difference with an active feedback loop by applying an interferometric in-loop reference. The reference interference spectrum shows a mitigated bandwidth because of spectral shaping of the seed pulses for precompensation of gain-narrowing. The stabilization strongly reduces the phase slip drift and thus leads to a stable burst spectrum over an extended time period.
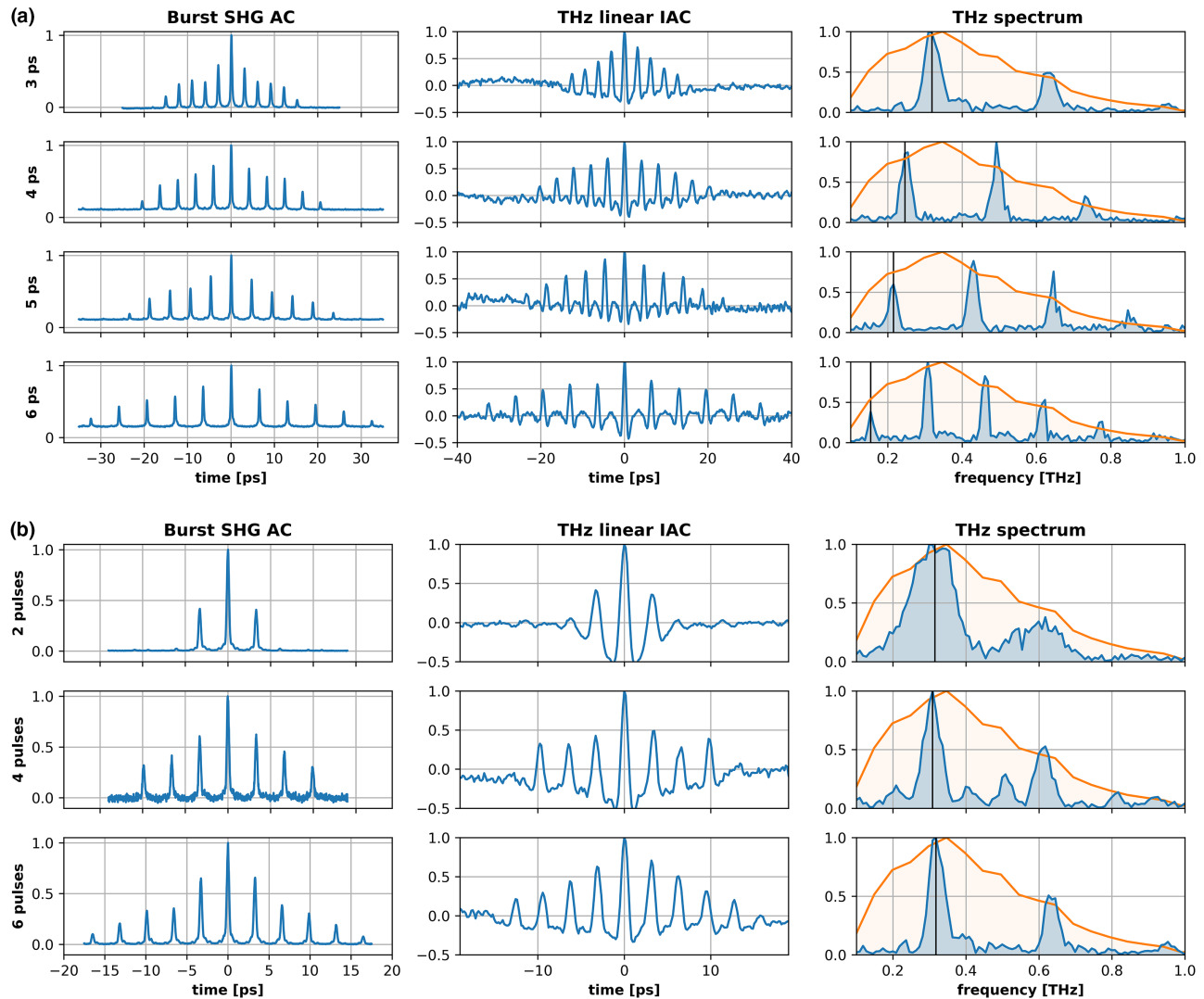
Fig. 6. Demonstration of control over THz intraburst repetition rates by generation of continuously tunable narrowband THz pulse bursts. Bursts of THz pulses are generated by driving a $LiNbO_3$ crystal with the NIR bursts. Second-harmonic autocorrelations of the NIR bursts (left) and linear interferometric autocorrelations from the THz pulse bursts (middle) were measured. Harmonic THz spectra (right) were retrieved from the latter by Fourier transformation, which are shown (blue) in comparison to the spectrum of a single THz pulse (orange). (a) Continuously tunable THz frequencies can be seen when varying the intraburst pulse spacing with a constant number of $N = 6$ pulses. (b) Controllable bandwidths of the THz peaks can be seen when varying the number of pulses with a constant intraburst pulse spacing Δt of 3 ps. Black vertical lines in the THz spectra indicate the intraburst repetition rates.

4. CONCLUSIONS

In conclusion, we demonstrate CPA of femtosecond pulse bursts with THz intraburst repetition rate to multi-mJ energies by directly controlling individual intraburst pulse phases, boosting the extractable energy of a chirped pulse amplifier in burst mode. Control over intraburst phase drift effects is implemented via an active feedback control loop that is conceptually similar to CEP stabilization developed earlier for continuous pulse trains [23] but is easier to apply because of a simple reference based on linear spectral interference. The developed laser source is shown to be an efficient driver for nonlinear optical applications such as tunable narrowband THz generation via optical rectification. Programmable intense THz pulse bursts can be applied to efficiently drive compact electron accelerators [28], enhance tailored nonlinear response of molecular gases via rotational stimulation [29], enable scanning-frequency THz spectroscopy, as well as to be used in arbitrary burst applications that

are sensitive to the fundamental-frequency pulse envelope but not to its phase. Further, we note that our method is suitable for various CPA layouts and gain materials. While this work is focused on suppressing spectral modes to extract more energy for a certain temporal burst shape, by turning off phase-scrambling and retaining intraburst phase stabilization, we directly obtain a highly promising source of NIR frequency combs [30] that offer interesting opportunities for high-acquisition-rate comb spectroscopies.

Note Added in Proof. While the paper was already in production, the phase slip stabilization technique was significantly improved by replacing the use of a reference beam with detection and evaluation of the burst buildup signal leaking through the reference-coupling TFP of the Vernier RA. This also allows extraction of the cavity round-trip detuning information. By that, the complexity of implementation is drastically reduced and the out-of-loop fidelity is highly improved.

Disclosures. The authors declare no conflicts of interest.

See Supplement 1 for supporting content.

[†] These authors contributed equally to this work.

REFERENCES

1. C. Kerse, H. K. Lu, P. Elahi, B. Çetin, D. K. Kesim, Ö. Akçaalan, S. Yavaş, M. D. Aşlk, B. Öktem, H. Hoogland, R. Holzwarth, and F. Ö. Ilday, "Ablation-cooled material removal with ultrafast bursts of pulses," Nature **537**, 84–88 (2016).
2. M. Murakami, B. Liu, Z. Hu, Z. Liu, Y. Uehara, and Y. Che, "Burst-mode femtosecond pulsed laser deposition for control of thin film morphology and material ablation," Appl. Phys. Express **2**, 042501 (2009).
3. V. N. Lednev, S. M. Pershin, P. A. Sdvizhenskii, M. Y. Grishin, M. A. Davydov, A. Y. Stavertiy, and R. S. Tretyakov, "Laser induced breakdown spectroscopy with picosecond pulse train," Laser Phys. Lett. **14**, 026002 (2017).
4. A. Willner, F. Tavella, S. Düsterer, B. Faatz, J. Feldhaus, H. Schlarb, S. Schreiber, S. Hädrich, J. Limpert, J. Rothhardt, E. Seise, A. Tünnermann, and J. Rossbach, "High repetition rate seeding of a free-electron laser at DESY Hamburg," in *Proc. IPAC* (2010).
5. B. Thurow, N. Jiang, M. Samimy, and W. Lempert, "Narrow-linewidth megahertz-rate pulse-burst laser for high-speed flow diagnostics," Appl. Opt. **43**, 5064–5073 (2004).
6. B. S. Thurow and A. Satija, "Design of a MHz repetition rate pulse burst laser system at Auburn University," in *44th AIAA Aerosp. Sci. Meet. Exhib.* (2006), pp. 1–11.
7. P. Wu, W. R. Lempert, and R. B. Miles, "Megahertz pulse-burst laser and visualization of shock-wave/boundary-layer interaction," AIAA J. **38**, 672–679 (2000).
8. C. Froehly, B. Colombeau, and M. Vampouille, "Shaping and analysis of picosecond light pulses," Prog. Opt. **20**, 63–153 (1983).
9. A. M. Weiner, "Femtosecond pulse shaping using spatial light modulators," Rev. Sci. Instrum. **71**, 1929–1960 (2000).
10. T. Kurokawa, H. Tsuda, K. Okamoto, K. Naganuma, H. Tenouchi, Y. Inoue, and M. Ishii, "Time-space-conversion optical signal processing using arrayed-waveguide grating," Electron. Lett. **33**, 1890–1891 (1997).
11. D. E. Leaird, A. M. Weiner, A. Sugita, S. Kamei, M. Ishii, and K. Okamoto, "Generation of high-repetition-rate WDM pulse trains from an arrayed-waveguide grating," IEEE Photon. Technol. Lett. **13**, 221–223 (2001).
12. D. E. Leaird, A. M. Weiner, S. Kamei, M. Ishii, and A. Sugita, "Generation of flat-topped 500-GHz pulse bursts using loss engineered arrayed waveguide gratings," IEEE Photon. Technol. Lett. **14**, 816–818 (2002).
13. D. E. Leaird and A. M. Weiner, "Femtosecond direct space-to-time pulse shaping in an integrated-optic configuration," Opt. Lett. **29**, 1551–1553 (2004).
14. J. A. Fülöp, Z. Major, B. Horváth, F. Tavella, A. Baltuška, and F. Krausz, "Shaping of picosecond pulses for pumping optical parametric amplification," Appl. Phys. B **87**, 79–84 (2007).
15. M. Barkauskas, K. Neimontas, and V. Butkus, "Device and method for generation of high repetition rate laser pulse bursts," WO patent 2018207042, UK patent 2562236 (15 November 2018).
16. I. Astrauskas, E. Kaksis, T. Flöry, G. Andriukaitis, A. Pugžlys, A. Baltuška, J. Ruppe, S. Chen, A. Galvanauskas, and T. Balčiūnas, "High-energy pulse stacking via regenerative pulse-burst amplification," Opt. Lett. **42**, 2201–2204 (2017).
17. S. Zhou, F. W. Wise, and D. G. Ouzounov, "Divided-pulse amplification of ultrashort pulses," Opt. Lett. **32**, 871–873 (2007).
18. M. Kienel, A. Klenke, T. Eidam, M. Baumgartl, C. Jauregui, J. Limpert, and A. Tünnermann, "Analysis of passively combined divided-pulse amplification as an energy-scaling concept," Opt. Express **21**, 29031–29042 (2013).
19. Y. Zaouter, F. Guichard, L. Daniault, M. Hanna, F. Morin, C. Hönninger, E. Mottay, F. Druon, and P. Georges, "Femtosecond fiber chirped- and divided-pulse amplification system," Opt. Lett. **38**, 106–108 (2013).
20. R. Byrd, P. Lu, J. Nocedal, and C. Zhu, "A limited memory algorithm for bound constrained optimization," J. Sci. Comput. **16**, 1190–1208 (1995).
21. A. Baltuška, T. Udem, M. Uiberacker, M. Hentschel, E. Goulielmakis, C. Gohle, R. Holzwarth, V. S. Yakovlev, A. Scrinzi, T. W. Hänsch, and F. Krausz, "Attosecond control of electronic processes by intense light fields," Nature **421**, 608–611 (2003).
22. G. Cerullo, A. Baltuška, O. D. Mücke, and C. Vozzi, "Few-optical-cycle light pulses with passive carrier-envelope phase stabilization," Laser Photon. Rev. **5**, 323–351 (2011).
23. G. Steinmeyer, B. Borchers, and F. Lücking, "Carrier-envelope phase stabilization," in *Progress in Ultrafast Intense Laser Science*, Vol. **IX**, (Springer, 2013), pp. 89–110.
24. J. Hebling, G. Almasi, I. Kozma, and J. Kuhl, "Velocity matching by pulse front tilting for large area THz-pulse generation," Opt. Express **10**, 1161–1166 (2002).
25. J. A. Fülöp, L. Pálfalvi, G. Almási, and J. Hebling, "Design of high-energy terahertz sources based on optical rectification," Opt. Express **18**, 4439–4444 (2010).
26. K. Lo Yeh, J. Hebling, M. C. Hoffmann, and K. A. Nelson, "Generation of high average power 1 kHz shaped THz pulses via optical rectification," Opt. Commun. **281**, 3567–3570 (2008).
27. P. S. Nugraha, G. Krizsán, G. Polónyi, M. I. Mechler, J. Hebling, G. Tóth, and J. A. Fülöp, "Efficient semiconductor multicycle terahertz pulse source," J. Phys. B **51**, 094007 (2018).
28. E. A. Nanni, W. R. Huang, K. H. Hong, K. Ravi, A. Fallahi, G. Moriena, R. J. Miller, and F. X. Kärtner, "Terahertz-driven linear electron acceleration," Nat. Commun. **6**, 8486 (2015).
29. S. Fleischer, R. W. Field, and K. A. Nelson, "Commensurate two-quantum coherences induced by time-delayed THz fields," Phys. Rev. Lett. **109**, 123603 (2012).
30. N. Picqué and T. W. Hänsch, "Frequency comb spectroscopy," Nat. Photonics **13**, 146–157 (2019).